Denaturant-Assisted Formation of a Stabilizing Disulfide Bridge from Engineered Cysteines in Nonideal Conformations†

Martin Karlsson, Lars-Göran Mårtensson, Carin Karlsson, and Uno Carlsson*

IFM-Department of Chemistry, Linköping University, SE-581 83 Linköping, Sweden

Received July 1, 2004; Revised Manuscript Received December 10, 2004

ABSTRACT: The engineered disulfide bridge A23C/L203C in human carbonic anhydrase II, inserted from homology modeling of *Neisseria gonorrhoeae* carbonic anhydrase, significantly stabilizes the native state of the protein. The inserted cysteine residues are placed in the interior of the structure, and because of the conformationally restrained localization, the protein is expressed in the reduced state and the cysteines are not readily oxidized. However, upon exposure to low concentrations of denaturant (0.6 M guanidine hydrochloride), corresponding to the lower part of the denaturation curve for the first unfolding transition, the oxidation rate of correctly formed disulfide bridges was markedly increased. By entropy estimations it appears that the increased flexibility, induced by the denaturant, enables the cysteines to find each other and hence to form the disulfide bridge. The outlined strategy of facilitating formation of disulfide bonds by addition of adjusted concentrations of a denaturant should be applicable to other proteins in which engineered cysteine residues are located in nonideal conformations. Moreover, a S99C/V242C variant was constructed, in which the cysteine residues are located on the surface. In this mutant the disulfide bridge was spontaneously formed and the native state was considerably stabilized (midpoint concentration of unfolding was increased from 1.0 to 1.4 M guanidine hydrochloride).

Proteins are useful for therapeutical or biotechnological applications only if they are stable enough to be produced, isolated, and stored. Several environmental factors such as temperature, pH, pressure, and denaturing agents can influence the protein stability. Since proteins are biologically active only when native, one important goal of protein engineering is to find ways to enhance the stability of proteins. The stabilizing factors in the native protein are the secondary and tertiary interactions, such as van der Waals interactions, hydrogen bonds, and salt bridges. In some proteins there are also covalent bonds between cysteine residues, disulfide bridges, which stabilize the structure. One possible way of increasing the global stability is therefore to engineer disulfide bonds into a protein of known structure (*1*). This is rather straightforward on the surface of proteins. However, in some cases it is not desirable to alter exposed amino acids. It is then preferable to engineer the disulfide bond into the interior of the protein, which is an objective that is more difficult to achieve because of the more conformationally restrained environment in the protein interior. In wild-type proteins, disulfide bond formation and the creation of structure are thermodynamically linked (*2*). Disulfide bonds stabilize the protein by restraining the unfolded state and thereby reducing the entropy loss upon refolding (*3*). The maximum entropic stabilization that can be achieved depends on the length of the loop between the cysteines; the longer between the cysteines in the primary structure, the more stabilizing the bridge will be (*4*−*6*). The gained stability by disulfide bridges is estimated to be in the order of 2.5−3.5 kcal/mol at 298 K (*7*). When a new disulfide bond is introduced into a protein, the stability rarely increases as much as predicted. This may be due to several factors that must be subtracted from the theoretical value. One reason can be that the replaced amino acids contributed to the protein stabilization. Another reason can be that the cysteines are not optimally placed with respect to each other, which can induce a slight strain in the molecule (*7*). To form a disulfide bond, the distance between the C_αs should be within 4.8−7.0 Å (*8*) and the side-chain environment should be such that they are conformationally able to permit the disulfide bond to adopt a torsional angle of 90° or −90°.

Besides the thermodynamic stabilization of proteins, introduction of disulfide bridges into proteins can render them less susceptible to proteolytic degradation by restraining otherwise flexible loops. Furthermore, introduction and analysis of engineered disulfide bridges can provide valuable information on protein folding (*9*) and protein dynamics (*10*) and can be used to suppress aggregation-prone intermediates (*11*).

Low-molecular-weight thiols such as reduced and oxidized glutathione or dithiothreitol are frequently used for the formation of nonnative disulfide bonds (*12*). However, if the two cysteines that are to be oxidized are buried within the protein structure, the reagent will not be able to oxidize the cysteine pair. In our ongoing studies on folding and stability we have earlier, by homology modeling using *Neisseria gonorrhoeae* carbonic anhydrase (NGCA) as a template, constructed the remarkably stable double cysteine mutant A23C/L203C of human carbonic anhydrase II (HCA II)[1] (*13*). NGCA has an extremely stabilizing disulfide bridge

† This work was supported by the Swedish Research Council (U.C. and L.-G.M.) and Stiftelsen Lars Hiertas Minne (M.K.).

* To whom correspondence should be addressed: e-mail ucn@ifm.liu.se; phone +46 13 281714; fax +46 13 281399.

10.1021/bi048610p CCC: $30.25
Published on Web 02/10/2005

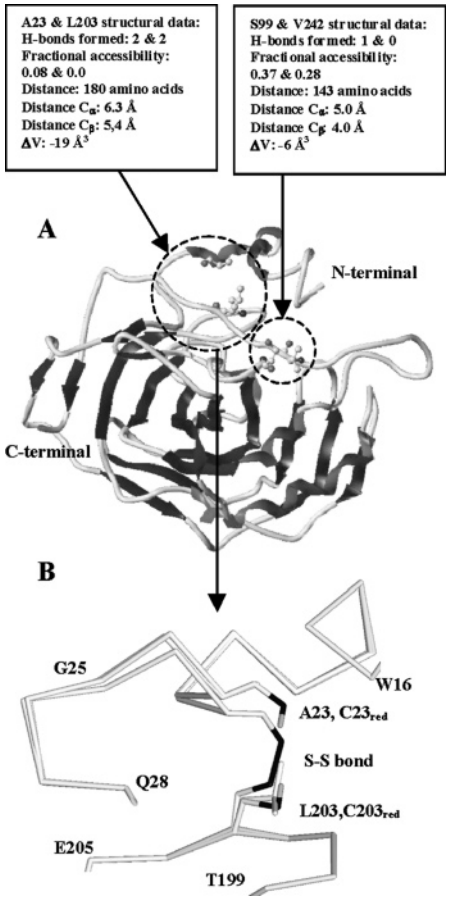

FIGURE 1: (A) Overall structure of HCA II (PDB 2cba) with the sites for introducing disulfide bridges indicated. The S−S bridge from S99C/V242C locks the long C-terminal loop to β-strand 4, and that of A23C/L203C locks the N-terminal domain. The boxes give information on the number of hydrogen bonds formed by the wild-type amino acids to be replaced, and the fractional solvent-accessible surfaces (*32*) of these residues. The distances in amino acid sequence between the wild-type amino acids to be mutated as well as the distances between the C_α and C_β atoms of these residues are also given. The differences in volume (ΔV) between the original amino acid pair and the replacing cysteines, obtained by use of earlier calculated side-chain volumes (*33*), are shown. (B) Detail of the wild-type structure of HCA II, the modeled structure of A23C/L203C$_{red}$ and A23C/L203C$_{ox}$, showing the C_α trace and the side chains in position 23 and 203. The hydrogen atoms are not shown except for the thiol groups of C23 and C203. The sulfur atoms are in dark gray.

(*14*), C28−C181, that corresponds to the buried residues Ala23 and Leu203 in HCA II. Thus, these positions were good candidates for engineering of a disulfide bond. This variant of HCA II is interesting in that it is expressed in the reduced form and does not spontaneously form a disulfide bond (Figure 1). However, this had the effect that the production of the oxidized variant was very tedious and time-demanding, because even at pH 8.5 with excess oxidizing agent (glutathione) the process is very slow, taking sometimes weeks of incubation to form 100% oxidized protein. Furthermore, in some preparations it was not possible to yield a fully oxidized protein. During stability studies of the reduced variant of A23C/L203C it was observed that the cysteine residues tended to oxidize more effectively upon exposure to moderate concentrations of the denaturant guanidine hydrochloride (GuHCl), which necessitated the addition of reduced DTT in the stability measurements of this variant (*13*). This indicates that the amino acids 23 and 203 are not optimally positioned in relation to each other in the 3D structure of the reduced form to build a covalent bond. The aim of this project was to produce the A23C/L203C variant of HCA II and an additional disulfide bridge variant of HCA II, where the cysteines to be oxidized are more exposed, to analyze their (i) contribution to the stability and (ii) disulfide bridge formation behavior.

MATERIALS AND METHODS

Molecular Modeling of the Side-Chain Conformations of A23C and L203C. The atomic coordinates of HCA II (PDB 2cba) was imported to the SYBYL software (Tripos Inc.) on a Silicon Graphics workstation, and the residues at positions A23 and L203 were mutated into cysteines. All hydrogens were added to the structure and the protein was assigned all Kollman charges. Side-chain conformations within the available space were systematically analyzed by a grid search method in two steps to avoid a combinatorial explosion. First, the combinations of χ_1 torsional angles of C23 and C203 were analyzed by exploring angles between 0° and 300° in steps of 60° and the energy was minimized for each of the 49 produced conformations. In most of the low-energy conformations the torsion angle of C203 was the same (−53°). The combination of C23 and C203 χ_1 torsional angles that gave the lowest energy was used in a second systematic search, where the combinations of χ_1 and χ_2 torsional angles of C23 were analyzed. All energy minimizations (Powell, convergence at 0.05 kcal/mol) were done with the Tripos force field with a distance-dependent dielectric constant of 4.0; all other settings were default. The energy was evaluated between the two cysteines and between the two cysteines and the rest of the protein treated as an aggregate. The structure with the lowest energy out of the 36 conformations produced for the C23 search was further analyzed by energy minimization of the reduced and oxidized forms of the structure obtained, by use of the same subset of amino acids as previously described (*13*).

Chemicals. Guanidine hydrochloride (GuHCl) was obtained from Pierce and was of reagent grade. The concentration was determined by refractive index (*15*). 7-Chloro-4-nitrobenzofurazan (NBD-Cl) was purchased from Fluka. All other chemicals used were of analytical grade.

Design of Surface-Located Disulfide Bridge Mutant. The program SSBOND (*16*) was employed in order to find candidate amino acids to change into cysteines that were supposed to form surface-located disulfide bridges. The positions found by the program were further analyzed by molecular graphics by use of the biopolymer module in the program SYBYL (Tripos Inc.).

Site-Directed Mutagenesis and Protein Expression and Purification. To avoid any unwanted disulfide bridges, the

[1] Abbreviations: A23C/L203C$_{ox}$ and A23C/L203C$_{red}$, oxidized and reduced forms, respectively, of pseudo-wild-type human carbonic anhydrase II with a Cys206 → Ser mutation with the additional mutations Ala23 → Cys and Leu203 → Cys; DTT$_{ox}$ and DTT$_{red}$, oxidized and reduced dithiothreitol, respectively; GuHCl, guanidine hydrochloride; HCA II$_{pwt}$, pseudo-wild-type human carbonic anhydrase II with a Cys206 → Ser mutation; NBD-Cl, 7-chloro-4-nitrobenzofurazan; S99C/V242C$_{ox}$ and S99C/V242C$_{red}$, oxidized and reduced forms, respectively, of pseudo-wild-type human carbonic anhydrase II with a Cys206 → Ser mutation with the additional mutations Ser99 → Cys and Val242 → Cys.

mutants (A23C/L203C and S99C/V242C) were produced in the pseudo-wild-type variant of HCA II (HCA II_{pwt}) containing the mutation C206S, as described earlier (*13*). This pseudo-wild-type form of the enzyme is functionally and structurally indistinguishable from the wild-type form (*17*) and its stability toward denaturation is practically identical (*18*). In an attempt to produce S99C/V242C in both reduced and oxidized forms, after affinity chromatography, the solution containing the S99C/V242C variant was divided into two approximately equal volumes, where one volume was dialyzed against 10 L of 10 mM Tris-H_2SO_4, pH 7.5, and the other volume was dialyzed against 10 L of 10 mM sodium borate buffer, pH 8.5. This was to see whether the disulfide bond was more efficiently formed when the pH was raised. The dialysis buffers were changed four times with at least 7 h in between. As there were some disulfide bridges (approximately 5−10%) formed in the preparation of the A23C/L203C variant, the protein was prepared as described before (*13*) with the exception that all solutions were degassed and supplemented with approximately 10 mM reduced DTT until the dialysis step. The exact concentration of enzyme was measured spectrophotometrically with the molar extinction coefficient at 280 nm (54 800 $M^{-1}\cdot cm^{-1}$) for HCA II (*19*).

Neisseria gonorrhoeae carbonic anhydrase (NGCA) was expressed in *Escherichia coli* as described by Chirica et al. (*20*).

Titration of Free Thiols. The content of free thiols was analyzed by labeling with NBD-Cl by incubation (5 min) of 17 μM protein, 5 M GuHCl, and 0.1 M Tris-H_2SO_4, pH 7.5. A 10-fold molar excess of NBD-Cl was added, after which the thiol modification reaction was allowed to proceed for 30 min at room temperature and monitored spectrophotometrically. The extent of NBD-Cl labeling was determined by absorbance measurement with the molar extinction coefficient at 420 nm (13 000 M^{-1} cm^{-1}) for the NBD−sulfur adduct (*21*).

Near-UV CD Measurements. Near-UV CD spectra were recorded on a CD6 spectrodichrograph (Jobin-Yvon Instruments) on the S99C/V242C enzyme variant (17 μM) by scanning the protein in both reduced and oxidized states, formed by overnight incubation in a 100-fold molar excess of DTT_{red} and DTT_{ox}, respectively. The protein was buffered with 10 mM Tris-H_2SO_4, pH 7.5, and a 5-mm quartz cell was used. A spectrum of the reference solution was subtracted from the protein spectrum.

Enzyme Activity Measurements. The esterase activity was measured according to Armstrong et al. (*22*) with *p*-nitrophenyl acetate (pNPA) as a substrate. The enzyme (0.85 μM) was buffered in 50 mM Tris-H_2SO_4, pH 8.5, and 0.1 M Na_2SO_4.

Stability Measurements. Stability analyses were made on a Hitachi F-4500 spectrofluorometer by following the spectral red shift of the intrinsic tryptophan fluorescence upon increasing concentrations of GuHCl. A number of samples of S99C/V242C were incubated overnight in different concentrations of GuHCl (0−6 M) in 0.1 M Tris-H_2SO_4, pH 7.5. A 1000-fold molar excess of DTT_{red} or a 100-fold molar excess of DTT_{ox} was added to form the reduced and oxidized states, respectively. Three fluorescence spectra (310−410 nm) of each sample were recorded after excitation at 295 nm with 5-nm excitation and emission slits, at 23 °C in a 1-cm quartz cuvette. The GuHCl midpoint concentration of unfolding (C_M) was calculated by a nonlinear least-squares fitting equation (*23*), with the program TableCurve 2D (Jandel Scientific).

Analysis of Disulfide Bond Formation. The quantification of disulfide bond formation was done by NBD-Cl (see above). The A23C/L203C_{red} protein variant (68 μM) was incubated for 20 h before analysis in increasing concentrations of GuHCl, at pH 7.5 and 8.5, with and without a 100-fold molar excess of the oxidizing agent DTT_{ox}.

SDS−PAGE Analysis. The monomeric status of A23C/L203C incubated in various concentrations of GuHCl was analyzed by SDS−PAGE. The protein (68 μM) in 10 mM borate buffer, pH 8.5, with a 100-fold molar excess of DTT_{ox}, was incubated for 20 h at different concentrations of GuHCl. The samples were desalted by microdialysis (Pierce) over a dialysis filter with a molecular weight cutoff of 10 000 (Millipore). SDS−PAGE was then performed on each sample (∼30 μg) under nonreducing conditions.

Analysis of Time Course of Disulfide Bridge Formation. The A23C/L203C_{red} variant (68 μM) was incubated in 10 mM borate buffer, pH 8.5, and a 100-fold molar excess of DTT_{ox} supplemented with 0.6 M GuHCl. Aliquots of the solution were, at different times, withdrawn and the content of free thiol groups was analyzed by NBD-Cl titration, as described above. As a reference the same experiment was repeated on an identical sample, without GuHCl.

Unfolding Entropy Change Determination. Solutions of 0.85 μM A23C/L203C_{red} in 0.1 M MOPS [3-(*N*-morpholino)-propanesulfonic acid], pH 7.5, with and without 0.6 M GuHCl were prepared and kept on ice. Aliquots (1.6 mL) were transferred from the solution to a thermostated cuvette. The time to reach unfolding equilibrium was established by monitoring the change in fluorescence intensity at 336 nm at each temperature, and for each temperature a fresh sample was incubated in order to prevent any problems with aggregation during incubation. After the sample had equilibrated, the intrinsic Trp fluorescence wavelength maximum was determined as described above. Measurements were performed on a Fluoromax-2 spectrofluorometer (Jobin-Yvon Instruments). The excitation wavelength was 295 nm and the excitation and emission slits were 3 and 4 nm, respectively. The fraction of unfolded protein was calculated from the fluorescence data and plotted as a function of temperature. The transition curves were obtained from nonlinear least-squares analysis (*23*). ΔG of unfolding was calculated for each temperature in the unfolding transition, assuming a two-state unfolding model. ΔS of unfolding was determined from the slope of the temperature dependence of ΔG. The data were fitted by linear regression. In an additional experiment the reversibility of the unfolding/refolding process was analyzed. A Trp fluorescence spectrum was first recorded at 20 °C below the T_m value of heat denaturation in the absence and presence of GuHCl (0.6 M; see Figure 6). The temperature was then raised to 20 °C above the T_m value and the time to reach unfolding equilibrium (approximately 6 min) was monitored as described above; the sample was then cooled to the starting temperature, while the fluorescence signal was monitored at 336 nm. When equilibrium was reached (1 h), a spectrum of the refolded protein was registered and the refolding yield was calculated from the difference in fluorescence wavelength maximum of native

Table 1: Side-Chain Torsional Angles and Distances in Wild-Type HCA II, Modeled Reduced and Oxidized A23C/L203C, and Wild-Type NGCA

protein variant	distance C_α (Å)	distance C_β (Å)	distance S−S (Å)	χ_1 (deg)	χ_2 (deg)	χ_3 (deg)
L203				−55	−73	
A23/L203	6.3	5.2				
$C23/C203_{red}$	6.3	5.5	4.5	C23, −62; C203, −63	C23, −61; C203, −180	
$C23/C203_{ox}$	5.3	4.0	2.0	C23, −56; C203, −67	C23, −71; C203, 148	94
NGCA	5.1	3.9	2.0	C28, −63; C181, −53	C28, −63; C181, 110	94

(335.5 nm) and refolded protein relative to the fluorescence maximum of unfolded protein (345 nm).

RESULTS AND DISCUSSION

A23C/L203C Mutant. The disulfide bond present in *Neisseria gonorrhoeae* carbonic anhydrase (NGCA) was recently grafted into structurally equivalent positions in human carbonic anhydrase II (HCA II, positions 23 and 203, Figure 1A), which led to a dramatic stabilization of the native structure. The A23C/L203C mutant was, however, expressed in *E. coli* in reduced form and the disulfide bridge was formed first after prolonged treatment with an oxidizing agent (oxidized glutathione) (*13*). On the contrary, the corresponding disulfide bridge in NGCA was spontaneously formed when also expressed in *E. coli*. This indicates that the engineered Cys residues are not optimally located in the HCA II structure. From the X-ray structures the $C_\alpha-C_\alpha$ distance between the two Cys residues in NGCA is 5.1 Å (*24*), which is rather close to the average distance observed for a right-handed disulfide bond (5.4 Å) (*8*), whereas the $C_\alpha-C_\alpha$ distance between Ala23 and Leu203 in HCA II is longer (6.3 Å; *25*). Modeling and geometry optimization of the location of the Cys residues and disulfide bond in the reduced and oxidized form, respectively, of the A23C/L203C mutant (Figure 1B; Table 1) showed that the $C_\alpha-C_\alpha$ distance between the Cys residues was 6.3 Å in the reduced form and was shortened to 5.3 Å upon disulfide bridge formation. Moreover, the gap between the C_β atoms of the Cys residues in $A23C/L203C_{red}$ is 0.3 Å wider than between the corresponding wild-type residues. Creation of the disulfide bond led to a 1.5 Å shorter $C_\beta-C_\beta$ distance. In addition, the distance between the sulfur atoms in the free Cys residues was 4.5 Å, 2.5 Å longer than in the disulfide bond. Thus, the unwillingness of the A23C/L203C mutant to form a disulfide bond combined with the X-ray and modeled structural data suggest that these engineered Cys residues are not located in an ideal conformation for a disulfide linkage to occur. Furthermore, we checked whether programs designed to select appropriate positions for Cys replacements for introduction of disulfide bonds based on stereochemical criteria would find these positions. However, SSBOND (*16*), Disulfide by Design (*26*), and MODIP (*27*) did not select positions 23 and 203 as candidates for substitution, supporting the notion that a disulfide bridge is not easily built in this location because of structural constraints.

Design of a Surface-Located Disulfide Bridge Mutant. For comparative purposes we made an attempt to engineer a disulfide mutant of HCA II that had the introduced Cys residues in more favorable positions than in the A23C/L203C mutant in order to facilitate formation of the disulfide bridge. For guidance in the selection of suitable mutation sites, we used the SSBOND program (*16*). Of the 59 possible disulfide bridge positions suggested by the program SSBOND, only the ones fulfilling certain criteria were of interest: (i) The distance between the two residues in the primary sequence should be long enough to ensure that the protein was stabilized, if the disulfide bridge was formed. (ii) The volume and polarity of the replaced side chains should be as similar as possible to that of cysteine residues so that the introduction of the new amino acids does not reduce the stability of the protein. (iii) The locations should preferably be at or near the surface, which will likely give the introduced Cys residues the highest conformational freedom and might facilitate disulfide bridge formation. Besides the above criteria, certain structural features of HCA II need to be considered. For example, β-sheets 3−5 are stable even at very high denaturant concentrations (*28*), so it is less interesting to introduce disulfide bridges within these structural elements, although it might be possible to anchor other structures to this stable core of the protein. Furthermore, there are two *cis*-prolines in the protein (Pro-30 and Pro-202) (*25*), which most probably are best left undisturbed by point mutations. After structural analysis of the suggested disulfide bridge positions, the S99C/V242C variant was chosen (Figure 1A).

Expression and Purification of HCA II Mutants. Analysis by SDS−PAGE verified that the expressed HCA II mutants were pure after being chromatographed on an affinity gel. Titration of thiols with NBD-Cl showed that A23C/L203C was fully reduced after preparation and dialysis at pH 7.5. Interestingly, the S99C/V242C variant was, on the other hand, expressed to more than 90% in the oxidized form at both pH 7.5 and 8.5. This shows that programs such as SSBOND are able to select appropriate mutation sites for disulfide bond formation. On the other hand, the remarkably stable $A23C/L203C_{ox}$ variant was not identified by several programs, since the location of the amino acid side chains of A23 and L203 fall outside the defined stereochemical constraints. This means that one runs a risk of overlooking interesting positions to mutate into cysteines by solely relying on programs that make selections after stereochemical criteria. The cysteines in the S99C/V242C variant more readily form disulfide bridges, as compared to the A23C/L203C variant, probably because of the more peripheral locations in the protein structure, which give them more conformational freedom than in the more buried positions of the A23C/L203C variant.

Table 2: Enzyme Esterase Activity and Stability Data for GuHCl-Induced Unfolding of HCA II_{pwt} and Cys Mutants as Monitored by Intrinsic Tryptophan Fluorescence Measurements

protein	activity (%)	$C_{m,NI}$[a]	$C_{m,IU}$[a]	$C_{m,NU}$[a]
HCA II_{pwt}	100	1.0	1.9	
S99C/V242C_{red}	37	0.9	1.8	
S99C/V242$_{ox}$	50	1.4	2.1	
A23C/L203C_{red}[b]	32	0.7	1.8	
A23C/L203C_{ox}[b]	42			1.8

[a] $C_{m,NI}$, $C_{m,IU}$, and $C_{m,NU}$ represent the transition midpoint concentrations for the transitions from the native (N) to the intermediate state (I), from the intermediate (I) to the unfolded state (U), and from the native to the unfolded state, respectively. [b] Data taken from ref 13.

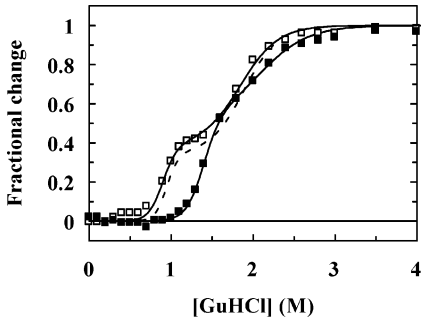

FIGURE 2: Protein stability curves of the S99C/V242C variant based on Trp fluorescence measurements at various concentrations of GuHCl: (□) reduced form; (■) oxidized form; (---) HCA II_{pwt} as a reference.

Structural and Functional Characterization. In the following, the S99C/V242C variant, that spontaneously forms a disulfide bridge, was characterized regarding stability and function and the A23C/L203C variant was used as a model for studies of denaturant-assisted formation of disulfide bridges. Near-UV CD spectra of the S99C/V242C variant were, in both the reduced and oxidized states, identical to those of HCA II, showing that the tertiary structure is intact (data not shown). The esterase activity was determined for the S99C/V242C mutant in both reduced and oxidized forms. To obtain both reduced and oxidized proteins, either DTT_{red} or DTT_{ox} was added to the protein samples. Although the esterase activity was decreased for all mutants, they are still catalytically relatively powerful (Table 2).

Stability toward GuHCl Denaturation. All protein variants of HCA II, except for A23C/L203C_{ox}, that have so far been engineered unfold via a stable molten globule intermediate and thereby unfold with two separate transitions. The unfolding reaction of A23C/L203C_{ox} appears to be a two-state process without the formation of the molten globule. However, previous studies have shown that a small fraction of an intermediate is formed also for A23C/L203C_{ox} (*13*). At a first glance, the S99C/V242C_{ox} variant also appears to unfold through a two-state process (Figure 2). However, this is due to the existence of a very small intermediate plateau. When the data are fitted to a three-state model, it is obvious that there are two processes taking place in the overall unfolding of this variant. The native state of S99C/V242C_{ox} is considerably more stable than that of HCA II_{pwt} (midpoint concentrations of unfolding at 1.4 and 1.0 M GuHCl, respectively; Table 2). The native states of the oxidized forms of A23C/L203C and S99C/V242C are the most stable variants of HCA II that have been produced to date. As can be seen from Figure 2 and Table 2, the native states of the

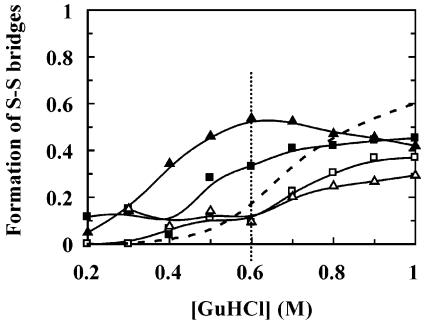

FIGURE 3: Relative formation of disulfide bridges in A23C/L203C in the presence of a denaturant. The measurements were performed after 20 h of incubation at different concentrations of GuHCl: (□) A23C/L203C at pH 7.5; (■) A23C/L203C, DTT_{ox} present at pH 7.5; (△) A23C/L203C at pH 8.5; (▲) A23C/L203C, DTT_{ox} present at pH 8.5. A normalized curve of the first unfolding transition (N → I) of A23C/L203C_{red}, adapted from Figure 3A in ref 13, is included for comparative purposes (---).

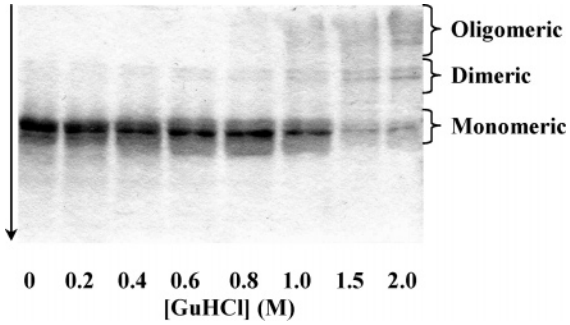

FIGURE 4: SDS−PAGE of reduced A23C/L203C after incubation at different concentrations of GuHCl. The samples were incubated for 20 h at pH 8.5 with a 100-fold molar excess of DTT_{ox}. The arrow indicates the migration direction.

reduced forms are less stable than that of HCA II_{pwt}. The fact that the reduced forms are less stable than the oxidized forms demonstrates that the formed disulfide bond is the stabilizing factor. The reduced S99C/V242C variant is less destabilized than the reduced A23C/L203C variant, which is likely due to the more flexible surface location of the mutagenesis sites and similar sizes of the replaced amino acid residues, minimizing imposed strain in the molecule. The much higher stability of the oxidized A23C/L203C mutant (3.7 and 6.6 kcal/mol stabilization of the native state compared to that of HCA II_{pwt} and A23C/L203C_{red}, respectively) might indicate that some perturbations in the reduced state are compensated for or restored in the oxidized state.

GuHCl Assistance in Disulfide Bond Formation in A23C/L203C. The contents of free SH groups were analyzed by NBD-Cl titration in order to follow the formation of the disulfide bond in the completely reduced A23C/L203C variant in the presence of varying concentrations of the denaturant GuHCl. The oxidation process was allowed to proceed for 20 h, with and without oxidizing agent (DTT_{ox}), at pH 7.5 and 8.5. The formation of disulfide bonds is shown in Figure 3, together with the first unfolding transition (native to molten globule state) of the reduced A23C/L203C as a reference. The amount of disulfide bridges formed at different GuHCl concentrations correlates rather well with the unfolding of the native state. At the onset of the unfolding transition (0.3−0.4 M GuHCl), low amounts of disulfide bridges are obtained at both pH 7.5 and 8.5. Below this GuHCl concentration no, or very low amounts of, disulfide bridges

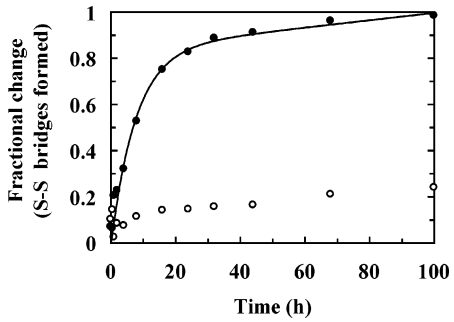

FIGURE 5: Time course of formation of disulfide bridges in A23C/L203C$_{red}$ in the presence and absence of GuHCl. The reaction was performed in 10 mM Tris-H_2SO_4, pH 8.5, supplemented with a 100-fold molar excess of DTT$_{ox}$. The data were best fitted to a single-exponential term (84%) followed by a small linear term. Symbols: (●) 0.6 M GuHCl, data and (—) fitted function; (○) 0 M GuHCl, data.

are formed within the reaction time. Presence of DTT$_{ox}$ facilitates disulfide formation, since more disulfide bridges are formed when a 100-fold molar excess of DTT$_{ox}$ is present. Noteworthy, at pH 8.5 in the presence of DTT$_{ox}$, there appears to be an optimal GuHCl concentration for disulfide bridge formation at approximately 0.6 M, just below the midpoint concentration of the first unfolding transition ($C_{m,NI}$ = 0.7 M GuHCl). This indicates that a certain increase in the flexibility of the protein structure is required for optimal conditions for disulfide formation induced by the denaturing agent. Beyond this point the protein structure probably will fluctuate too much for intramolecular bridge formation. The induced increased flexibility of the protein will, of course, also increase the accessibility of the buried Cys residues to the oxidizing agent.

SDS−PAGE Analysis. SDS−PAGE was used to investigate whether the disulfide bonds formed were intramolecular or intermolecular in character. A new series of samples were incubated for 20 h at various concentrations of GuHCl. As can be seen from the SDS−PAGE gel in Figure 4, only a minor fraction of the protein formed dimers at 0.6 M GuHCl, whereas there is a large increase of dimer and oligomer formation at 0.8 M and higher concentrations of GuHCl. In addition, it is interesting to observe that practically only dimers are formed at GuHCl concentrations inducing the molten globule state. This indicates that only one of the two cysteine residues is exposed in the molten globule intermediate.

Time Study of Disulfide Bridge Formation. Since incubation at 0.6 M GuHCl with a 100-fold molar excess of DTT$_{ox}$ at pH 8.5 gave the optimal conditions for disulfide bridge formation in A23C/L203C$_{red}$ with only low amounts of dimer formation, a time study was performed to follow the disulfide bridge formation from initiation to completion under these conditions. Figure 5 displays the large impact that a moderate concentration of the denaturant has on the kinetics of disulfide bridge formation in this protein variant. The disulfide bridge formation at 0.6 M GuHCl was best fitted to one exponential phase ($t_{1/2}$ = 5.4 h) followed by a small linear phase and reaches complete oxidation of the protein after approximately 4 days. At this point only about 25% of the protein incubated in a buffer lacking GuHCl has been oxidized, which clearly demonstrates that it is the denaturant that facilitates the formation of the disulfide bridges. This is, to our knowledge, the first example of acceleration of disulfide bridge formation of an internal cysteine pair by addition of moderate amounts of a denaturant. In an earlier work by Low et al. (*29*), it was shown that anions could accelerate oxidative folding of ribonuclease A by formation and stabilization of nativelike intermediates. Interestingly, by adding a moderate concentration of denaturant to a fully folded protein, as in this case, the same result is obtained by destabilization.

Unfolding Entropy Change of A23C/L203C$_{red}$. We have interpreted the more efficient formation of the disulfide bridge in the presence of GuHCl to be due to increased flexibility of the native structure. To obtain some supportive evidence of this, the entropy change of denaturation was determined in 0 and 0.6 M GuHCl by measuring the degree of unfolding for the A23C/L203C$_{red}$ variant as a function of temperature (Figure 6A). It should, however, be pointed out that the denaturation process of HCA II is not completely reversible due to some aggregation in the molten globule state (*30*, *31*). Because of the short exposure times at elevated temperature in these experiments, a high degree of reversibility was nevertheless obtained [84% and 87% recovery of the fluorescence wavelength maximum in 0 and 0.6 M GuHCl, respectively, upon heating and cooling to the temperatures giving rise to the plateau values (0 M GuHCl, 29 °C ↔ 69 °C; 0.6 M GuHCl, 6 °C ↔ 46 °C)]. Although absolute Δ*S* values cannot be accurately determined, it is reasonable to believe that most of the error caused by aggregation will be canceled out when, as in this case, the entropy change of the same protein is compared and only the trend in Δ*S* is of interest. From the temperature dependence of Δ*G*, the entropy changes were calculated to 1.1 and 0.8 kcal/mol in 0 and 0.6 M GuHCl, respectively

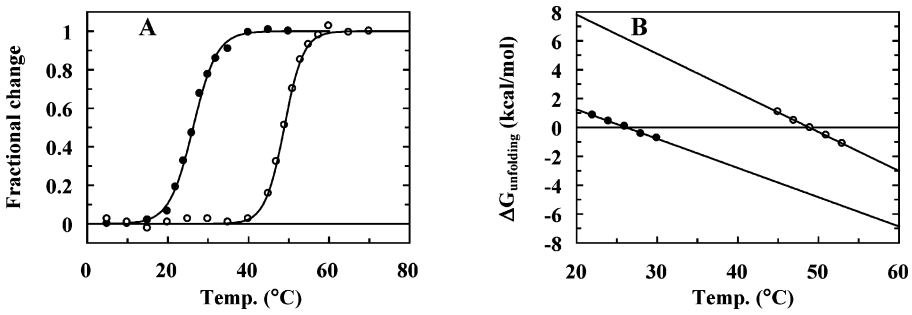

FIGURE 6: Stability toward thermal denaturation of A23C/L203C$_{red}$. The unfolding process was studied in 0.1 M MOPS buffer, pH 7.5, with (●) and without (○) 0.6 M GuHCl. (A) Degree of unfolding as measured by the shift in emission wavelength maximum of the intrinsic tryptophan fluorescence. The T_m values from these curves are 49 and 26 °C at 0 and 0.6 M GuHCl, respectively. (B) Δ*G* of unfolding calculated from the fraction of unfolded protein in the temperature transition zone. Δ*S* was obtained as the slope of the fitted linear function.

(Figure 6B). Thus, the entropic difference between the native and unfolded state is lower at 0.6 M GuHCl. If the unfolded state primarily is affected by the action of GuHCl (0.6 M), the entropic change of denaturation should be expected to increase upon going from 0 to 0.6 M GuHCl. Therefore, the observed decrease in ΔS on the contrary indicates that the protein is more flexible in the native state at 0.6 M GuHCl, supporting the idea that it is the increased flexibility of the protein in moderate concentration of GuHCl that enables the cysteines to find each other and hence form the disulfide bridge.

CONCLUDING REMARKS

In many applications it is valuable to find methods to speed up the formation of disulfide bridges in a protein or make it possible for them to form at all. This study shows that a protein with cysteine residues in nonideal positions, in a conformationally restrained environment, can be assisted to form disulfide bonds by the action of moderate concentrations of a denaturant. Both the yield of the disulfide bond bridges and the kinetics of formation are favorably affected by the denaturant. We suggest that this method of adding a denaturant, at a concentration corresponding to the lower part of the unfolding curve, can be generally used to facilitate formation of disulfide bridges by engineered cysteines in the interior of a protein, in particular when low or no yield of S−S bonds is obtained.

REFERENCES

1. Matsumura, M., and Matthews, B. W. (1991) Stabilization of functional proteins by introduction of multiple disulfide bonds, *Methods Enzymol. 202*, 336−356.
2. Gilbert, H. F. (1996) The formation of native disulfide bonds, in *Mechanism of protein folding* (Pain, R. H., Ed.) pp 104−131, Oxford University Press, Oxford, U.K.
3. Matsumura, M., Becktel, W., Levitt, M., and Matthews, B. W. (1989) Stabilization of phage T4 lysozyme by engineered disulfide bonds, *Proc. Natl. Acad. Sci. U.S.A. 86*, 6562−6566.
4. Flory, P. J. (1956) Theory of elastic mechanisms in fibrous proteins, *J. Am. Chem. Soc. 78*, 5222.
5. Abkevich, V. I., and Shakhnovich, E. I. (2000) What can disulfide bonds tell us about protein energetics, function and folding: simulations and bioinformatics analysis, *J. Mol. Biol. 300*, 975−985.
6. Mason, J. M., Gibbs, N., Sessions, R. B., and Clarke, A. R. (2002) The Influence of intramolecular bridges on the dynamics of a protein folding reaction, *Biochemistry 41*, 12093−12099.
7. Braxton, S. (1996) Protein Engineering for Stability, in *Protein engineering: Principles and practice* (Cleland, J. L., and Craik, C. S., Eds.) Wiley-Liss Inc., New York.
8. Petersen, M., Jonson, P. H., and Petersen, S. B. (1999) Amino acid neighbours and detailed conformational analysis of cysteines in proteins, *Protein Eng. 12*, 535−548.
9. Clarke, J., and Fersht, A. R. (1993) Engineered disulfide bonds as probes of the folding pathway of barnase−Increasing the stability of proteins against the rate of denaturation, *Biochemistry 32*, 4322−4329.
10. Butler, S. L., and Falke, J. J. (1996) Effects of protein stabilizing agents on thermal backbone motions: A disulfide trapping study, *Biochemistry 35*, 10595−10600.
11. Karlsson, M., Mårtensson, L.-G., Olofsson, P., and Carlsson, U. (2004) Circumnavigating misfolding traps in the energy landscape through protein engineering: suppression of molten globule and aggregation in carbonic anhydrase, *Biochemistry 43*, 6803−6807.
12. Rudolph, R. (1996) Successful Protein Folding on an Industrial scale, in *Protein engineering: Principles and practice* (Cleland, J. L., and Craik, C. S., Eds.) Wiley-Liss Inc., New York.
13. Mårtensson, L.-G., Karlsson, M., and Carlsson, U. (2002) Dramatic stabilization of the native state of human carbonic anhydrase II by an engineered disulfide bond, *Biochemistry 41*, 15867−15875.
14. Elleby, B., Chirica, L. C., Tu, L., Zeppezauer, M., and Lindskog, S. (2001) Characterization of carbonic anhydrase from *Neisseria gonorrhoeae*, *Eur. J. Biochem. 268*, 1613−1619.
15. Nozaki, Y. (1972) The preparation of guanidine hydrochloride, *Methods Enzymol. 26*, 43−50.
16. Hazes, B., and Dijkstra, B. W. (1988) Model building of disulfide bonds in proteins with known three-dimensional structure, *Protein Eng. 2*, 119−125.
17. Mårtensson, L.-G., Jonsson, B.-H., Andersson, M., Kihlgren, A., Bergenhem, N., and Carlsson, U. (1992) Role of an evolutionarily invariant serine for the stability of human carbonic anhydrase II, *Biochim. Biophys. Acta 1118*, 179−186.
18. Mårtensson, L.-G., Jonsson, B.-H., Freskgård, P.-O., Kihlgren, A., Svensson, M., and Carlsson, U. (1993) Characterization of folding intermediates of human carbonic anhydrase II: Probing substructure by chemical labeling of SH groups introduced by site-directed mutagenesis, *Biochemistry 32*, 224−231.
19. Nyman, P. O., and Lindskog, S. (1964) Amino acid composition of various forms of bovine and human erythrocyte carbonic anhydrase, *Biochim. Biophys. Acta 85*, 141−151.
20. Chirica, L. C., Elleby, B., Jonsson, B.-H., and Lindskog, S. (1997) The complete sequence, expression in *Escherichia coli*, purification and some properties of carbonic anhydrase from *Neisseria gonorrhoeae*, *Eur. J. Biochem. 244*, 755−760.
21. Birkett, D. J., Dwek, R. A., Radda, G. K., Richards, R. E., and Salmon, A. G. (1971) Probes for the conformational transitions of phosphorylase b. Effect of ligands studied by proton relaxation enhancement, fluorescence and chemical reactivities, *Eur. J. Biochem. 20*, 494−508.
22. Armstrong, J. M., Wyers, D. V., Verpoorte, J. A., and Edsall, J. T. (1966) Purification and properties of human erythrocyte carbonic anhydrases, *J. Biol. Chem. 241*, 5137−5149.
23. Santoro, M. M., and Bolen, D. W. (1988) A test of the linear extrapolation of unfolding free energy changes over an extended denaturant concentration range, *Biochemistry 27*, 8063−8068.
24. Huang, S., Xue, Y., Sauer-Eriksson, E., Chirica, L., Lindskog, S., and Jonsson, B.-H. (1998) Crystal structure of carbonic anhydrase from *Neisseria gonorrhoeae* and its complex with the inhibitor acetazolamide, *J. Mol. Biol. 283*, 301−310.
25. Håkansson, K., Carlsson, M., Svensson, L. A., and Liljas, A. (1992) Structure of native and apo carbonic anhydrase II and structure of some of its anion-ligand complexes, *J. Mol. Biol. 227*, 1192−1204.
26. Dombkowski, A. A. (2003) Disulfide by design: A computational method for the rational design of disulfide bonds in proteins, *Bioinformatics 19*, 1852−1853.
27. Sowdhamini, R., Srinivasan, N., Shoichet, B., Santi, D. V., Ramakrishnan, C., and Balaram P. (1989) Stereochemical modelling of disulfide bridges: Criteria for introduction into proteins by site-directed mutagenesis, *Protein Eng. 3*, 95−103.
28. Svensson, M., Jonasson, P., Jonsson, B.-H., Lindgren, M., Mårtensson, L.-G., Gentile, M., Borén, K., and Carlsson, U. (1995) Mapping the folding intermediate of human carbonic anhydrase II. Probing substructure by chemical reactivity and spin and fluorescence labeling of engineered cysteine residues, *Biochemistry 34*, 8606−8620.
29. Low, L. K., Shin, H.-C., Naryan, M., Wedemeyer, W. J., and Scheraga, H. A. (2000) Acceleration of oxidative folding of bovine pancreatic ribonuclease A by anion-induced stabilization and formation of structured nativelike intermediates, *FEBS Lett. 472*, 67−72.
30. Hammarström, P., Persson, M., Freskgård, P.-O., Mårtensson, L.-G., Andersson, D., Jonsson, B.-H., and Carlsson, U. (1999) Structural mapping of an aggregation nucleation site in a molten globule intermediate, *J. Biol. Chem. 274*, 32897−32903.
31. Hammarström, P., Persson, M., and Carlsson, U. (2001) Protein compactness measured by fluorescence resonance energy transfer. Human carbonic anhydrase II is considerably expanded by the interaction of GroEL, *J. Biol. Chem. 276*, 21765−21775.
32. Lee, B., and Richards, F. M. (1971) The interpretation of protein structures: Estimation of static accessibility, *J. Mol. Biol. 55*, 379−400.
33. Richards, F. M. (1974) The interpretation of protein structures: Total volume, group volume distributions and packing density, *J. Mol. Biol. 82*, 1−14.

BI048610P